



HAL
open science

Assessing Cardiac Amyloidosis Subtypes by Unsupervised Phenotype Clustering Analysis

Louis Bonnefous, Mounira Kharoubi, Mélanie Bézard, Silvia Oghina, Fabien Le Bras, Elsa Poullot, Valérie Molinier-Frenkel, Pascale Fanen, Jean-François Deux, Vincent Audard, et al.

► **To cite this version:**

Louis Bonnefous, Mounira Kharoubi, Mélanie Bézard, Silvia Oghina, Fabien Le Bras, et al.. Assessing Cardiac Amyloidosis Subtypes by Unsupervised Phenotype Clustering Analysis. *Journal of the American College of Cardiology*, 2021, 78 (22), pp.2177-2192. 10.1016/j.jacc.2021.09.858 . hal-04392277

HAL Id: hal-04392277

<https://hal.science/hal-04392277>

Submitted on 22 Jul 2024

HAL is a multi-disciplinary open access archive for the deposit and dissemination of scientific research documents, whether they are published or not. The documents may come from teaching and research institutions in France or abroad, or from public or private research centers.

L'archive ouverte pluridisciplinaire **HAL**, est destinée au dépôt et à la diffusion de documents scientifiques de niveau recherche, publiés ou non, émanant des établissements d'enseignement et de recherche français ou étrangers, des laboratoires publics ou privés.



Distributed under a Creative Commons Attribution - NonCommercial 4.0 International License

Assessing Cardiac Amyloidosis Subtypes by Unsupervised Phenotype Clustering Analysis

Brief title: Cardiac amyloidosis subtypes by unsupervised phenotype clustering.

Louis Bonnefous, PhD (c)^{1,2,3,4}, Mounira Kharoubi, PhD (c)^{2,3,4,5}, Mélanie Bézard, PhD (c)^{2,3,4,5}, Silvia Oghina, MD^{2,3,4,5}, Fabien Le Bras, MD^{2,3,6}, Elsa Poullot, MD^{2,7}, Valérie Molinier-Frenkel, MD, PhD^{2,4,7}, Pascale Fanen, MD, PhD^{2,4,8}, Jean-François Deux, MD, PhD^{2,3,4,9}, Vincent Audard, MD, PhD^{2,3,4,10}, Emmanuel Itti, MD, PhD^{2,3,4,11}, Thibaud Damy, MD, PhD^{2,3,4,5,12*}, Etienne Audureau, MD, PhD^{1,4*,**}

1 AP-HP (Assistance Publique-Hôpitaux de Paris), Public Health Department, Henri Mondor University Hospital, F-94010, Créteil, France

2 AP-HP (Assistance Publique-Hôpitaux de Paris), French Referral Centre for Cardiac Amyloidosis, Cardiogen Network, Henri Mondor University Hospital, F-94010, Créteil, France

3 AP-HP (Assistance Publique-Hôpitaux de Paris), GRC Amyloid Research Institute, Henri Mondor University Hospital, F-94010, Créteil, France

4 Univ Paris Est Creteil, INSERM, IMRB, F-94010 Créteil, France

5 AP-HP (Assistance Publique-Hôpitaux de Paris), Cardiology Department, Henri Mondor University Hospital, F-94010, Créteil, France

6 AP-HP (Assistance Publique-Hôpitaux de Paris), Hematology Department, Henri Mondor University Hospital, F-94010, Créteil, France

7 AP-HP (Assistance Publique-Hôpitaux de Paris), Biology-Pathology Department, Henri Mondor University Hospital, F-94010, Créteil, France,

8 AP-HP (Assistance Publique-Hôpitaux de Paris), Genetics Department, Henri Mondor University Hospital, F-94010, Créteil, France

9 AP-HP (Assistance Publique-Hôpitaux de Paris), Radiology Department, Henri Mondor University Hospital, F-94010, Créteil, France

10 AP-HP (Assistance Publique-Hôpitaux de Paris), Nephrology Department, Henri Mondor University Hospital, F-94010, Créteil, France

11 AP-HP (Assistance Publique-Hôpitaux de Paris), Nuclear Medicine Department, Henri Mondor University Hospital, F-94010, Créteil, France

12 AP-HP (Assistance Publique-Hôpitaux de Paris), Clinical Investigation Center 1430, Henri Mondor University Hospital, F-94010, Créteil, France

* These two authors equally contributed to this work.

**Corresponding author.

Data not available due to ethical restrictions: due to the nature of this research, participants of this study did not agree for their data to be shared publicly.

Funding: LB reports a PhD grant from GlaxoSmithKline.

Disclosures: SO received honoraria from Pfizer. TD received research and/or consultant fees from GlaxoSmithKline, Alnylam, Pfizer, Prothena, Ionis, Akcea and Janssen. EA reports consultant fees from GBT and Hemanext. The remaining authors have nothing to disclose.

Address for correspondence

Pr Etienne Audureau
Service de Santé Publique, Hôpital Henri Mondor
1 rue Gustave Eiffel, 94000 Créteil, France
Tel: +33(0)1.49.81.36.64
Fax: +33(0)1.49.81.36.97
etienne.audureau@aphp.fr

Twitter : @thibauddamy

Acknowledgments

The authors thank all patients and investigators at Mondor Amyloidosis Network, Henri Mondor University Hospital, for their important contributions to this study. We thank Laura Smales for editing the manuscript.

Abstract

Background: Cardiac amyloidosis (CA) is a set of amyloid diseases with usually predominant cardiac symptoms, including light-chain amyloidosis (AL), hereditary variant transthyretin amyloidosis (ATTRv) and wild-type transthyretin amyloidosis (ATTRwt). CA are characterized by high heterogeneity in phenotypes leading to diagnosis delay and worsened outcomes.

Objectives We used clustering analysis to identify typical clinical profiles in a large population of patients with suspected CA.

Methods: Data were collected from the French Referral Center for Cardiac Amyloidosis database (Hôpital Henri Mondor, Créteil), including 1394 patients with suspected CA between 2010 and 2018: 345 (25%) had a diagnosis of AL, 263 (19%) ATTRv, 402 (29%) ATTRwt and 384 (28%) no amyloidosis. Based on comprehensive clinico-biological phenotyping, unsupervised clustering analyses were performed by artificial neural network based self-organizing maps (SOMs) to identify patient profiles (clusters) with similar characteristics, independent of the final diagnosis and prognosis.

Results: Mean \pm standard deviation age and left ventricular ejection fraction were 72 ± 13 years and $52\%\pm 13$. We identified seven clusters of patients with contrasting profiles and prognosis. AL patients were distinctively located within a typical cluster; ATTRv patients were distributed across four clusters with varying clinical presentations, one of which overlapping with patients without amyloidosis; interestingly, ATTRwt patients spread across three distinct clusters with contrasted risk factors, biological profiles and prognosis.

Conclusions: Clustering analysis identified seven clinical profiles with varying characteristics, prognosis and associations with diagnosis. Especially in patients with ATTRwt, these results suggest key areas to improve amyloidosis diagnosis and stratify prognosis depending on associated risk factors.

Condensed abstract: Cardiac amyloidosis (CA) is characterized by high heterogeneity in phenotypes leading to diagnosis delay and worsened outcomes. Using clustering analysis by self-organizing maps in 1394 patients with suspected CA, we identified seven typical clinico-biological presentations. AL patients were distinctively located within a typical cluster; ATTRv patients were distributed across four clusters with varying clinical presentations, one of which overlapping with patients without amyloidosis; ATTRwt patients spread across three distinct clusters with contrasted risk factors, biological profiles and prognosis. Especially in patients with ATTRwt, these results suggest key areas to improve amyloidosis diagnosis and stratify prognosis depending on associated risk factors.

Keywords: Cardiac amyloidosis – Clustering - Phenotype - Diagnosis - Prognosis

Abbreviations

AL: light-chain amyloidosis

ATTRv: hereditary variant transthyretin amyloidosis

ATTRwt: wild-type transthyretin amyloidosis

CA: cardiac amyloidosis

SOMs: self-organizing maps

Introduction

Amyloidosis is a set of diseases caused by abnormal protein folding that generates insoluble fibrils within the extracellular matrix of tissues and organs(1). In total, 36 responsible proteins have been identified, but the most common types of amyloidosis are due to transthyretin (ATTR) or light chains of immunoglobulin (AL)(2). ATTR has two distinct forms: wild-type (ATTRwt) (also known as senile systemic amyloidosis) and hereditary (ATTRv). More than 100 pathogenic mutations in the *TTR* gene have been identified(3).

These three most common types of amyloidosis feature predominant heart manifestations, so they are part of the cardiac amyloidosis (CA) family. Patients typically display a phenotype of hypertrophic cardiomyopathy (HCM), associated with heart failure (HF) and poor prognosis(4). CA shares the same cardiac manifestations (dyspnea, atrial fibrillation) as other cardiac diseases, such as hypertensive heart disease (HHD) or heart failure with preserved ejection fraction (HFpEF)(5-7). However, CA patients also frequently present various other symptoms or “red flags” (8), which reflect the pathophysiology of the disease(8,9). Such extracardiac manifestations may notably include neurologic (i.e., peripheral neuropathy(10)), tegumentary (i.e., carpal tunnel syndrome, spinal stenosis, underlying Dupuytren syndrome(11,12)) and otorhinolaryngologic (hearing loss(13,14)) symptoms as well as skin or mucosal impairment (macroglossia, periorbital bruises, cutaneous purpura (15)).

Even though the diagnosis of ATTR-CA has become simpler thanks to bone tracer scintigraphy, the diagnosis of AL-CA can still be challenging and may rely on a complex combination of clinical, biological and imaging examinations(9). There is also clear heterogeneity of CA clinical expression and potential overlap with other cardiac conditions. Lack of awareness of such heterogeneity by clinicians may expose patients to under-, mis- or late

diagnosis resulting in delayed appropriate management and aggravated outcome(16). We need to improve our knowledge of the varying phenotypes of CA to better characterize them and help cardiologists identify less frequent presentations warranting thorough clinical and paraclinical examinations.

Clustering techniques based on machine learning algorithms and following an unsupervised (without *a priori* hypotheses) approach can reveal hidden commonalities or key differences and could help disentangle the CA heterogeneous clinical expressions(17).

The aim of this study was to identify and characterize clinical profiles within a mixed controls–CA population by using clustering analysis and to secondarily investigate the association of profiles with established CA diagnoses and their prognostic value for mortality.

Methods

Study population

Data were collected from the Referral Center for Cardiac Amyloidosis database, a cohort study of prospectively enrolled adult patients referred for suspected CA to the Henri Mondor University Hospital, Créteil, France. For the present analysis, the study population included all patients enrolled from 2010 to 2018 and for whom a definite diagnosis of CA was established (ATTRv/ATTRwt/AL) or discarded (controls); patients recently referred and still under investigation at the time of data extraction were not included.

The study was conducted according to the Declaration of Helsinki. Informed consent was collected from all patients before inclusion. The study was approved by the local ethics committee of Henri Mondor hospital and the French Data Protection Authority (Commission Nationale de l'Informatique et des Libertés; authorization no. 1431858).

Diagnostic criteria

Diagnosis of CA was considered when interventricular septum thickness measured by echocardiography was 12 mm (without another known cause) and/or cardiac MRI showed diffuse late gadolinium enhancement and/or ^{99m}Tc-bisphosphonate scintigraphy showed strong tracer uptake by the heart.

The types of amyloidosis had the following definitions. AL was diagnosed on the basis of high monoclonal light-chain levels in serum and/or urine and an extracardiac or endomyocardial biopsy showing both Congo red staining and labeling with specific anti-k or anti-light-chain antibodies. ATTR was diagnosed on the basis of cardiac fixation on bone scintigraphy without gammopathy. With the presence of gammopathy, a biopsy was performed (extracardiac and/or cardiac) with Congo red staining and anti-TTR antibody labelling without anti-light-chain antibody staining. Patients with ATTR underwent genetic analysis of the *TTR* gene to discriminate those with ATTRv (presence of a pathogenic mutation) and ATTRwt (no mutation).

Data collection

Baseline data were collected during routine clinical practice from an examination recommended for patients with suspected CA(9) and included demographic, clinical, biological, genetic and imaging findings measured at the time of enrolment in the study, considering the latest examinations/data available up to 6 months after the initial referral. For the present analysis, 24 features currently considered relevant for CA characterization were considered for the clustering analysis: demographics (age, sex), physical examination (body mass index [BMI]), New York Heart Association [NYHA] class, systolic blood pressure [SBP]), cardiovascular [CV] risk factors (hypertension, diabetes and dyslipidaemia), (para)clinical parameters commonly associated with amyloidosis (underlying gammopathy, myeloma and Waldenstrom pathology (18), hearing loss(13), soft tissue deposition(11), peripheral neuropathy(10), skin/mucosal

impairment(15), cardiac fixation on bone scintigraphy), biological parameters (N-terminal-pro-hormone B-type natriuretic protein [NTproBNP] and troponin measures(19), anemia and creatinine clearance), electrocardiography parameters (microvoltage and arrhythmia), and echocardiography parameters (heart rate, left ventricular ejection fraction [LVEF], global LV strain(19) and interventricular septum thickness [IST]); detailed definition criteria are given in **Supplemental Methods.**

Statistical analyses

The main part of the analysis sought to identify novel specific patient profiles to improve the characterization of CA by applying unsupervised (without *a priori* CA diagnosis) clustering analysis based on the 24 patient characteristics previously detailed, independent of the final diagnosis. Clustering analysis relied on building self-organizing maps (SOMs), a nonparametric approach based on Kohonen's neural networks allowing to convert multidimensional datasets with large numbers of variables into simplified grids displayed as 2-D maps(20).

In a nutshell, SOM algorithms assign each individual a specific area on the map based on their characteristics, placing similar individuals in close proximity and distinct ones in remote locations, thus allowing to draw visual comparisons of unique or overlapping patient characteristics and disease subtypes. The SOMs were constructed by applying the approach developed within the *Numero* package framework for the R statistical platform(21), by 1) building the SOMs with statistical verification of the robustness of the contrasts observed by permutation tests and 2) determining suitable groupings based on the direct visualization of data patterns and key characteristics of the dataset. A sensitivity analysis was conducted to check the robustness of the main findings obtained by SOMs, by following a model-based clustering approach with the *mclust* R package(22).

For illustrative purposes, Gabriel's biplots were plotted to project the patients along the principal components axes from mixed principal component analysis according to their individual characteristics, colouring patients according to their final diagnosis or cluster and thus allowing for direct visual assessment of the discriminative ability of each subgrouping.

Comparisons of clinical, biological, and cardiological features between groups involved one-way ANOVA or Kruskal-Wallis tests for continuous data and chi-square or Fisher's exact test for categorical data, as appropriate.

Survival analyses were performed to assess the prognostic value of the different subgroups identified on overall survival. Survival curves were plotted by the Kaplan-Meier method, using log-rank tests to assess significance for group comparison.

NTproBNP and troponin levels were log-transformed to account for data skewness. Among the 24 features used for clustering, missing rates ranged from 0% for most variables to 33% for cardiac fixation on bone scintigraphy; for the SOM analysis, those variables with missing information were imputed using the k-nearest neighbours (kNN) approach. Among the other variables used only as illustrative features, variables with missing rates >30% included electrocardiography-PR, -QRS, ethnic origin, dysphonia and orthostatic hypotension. All descriptive statistics are presented as raw (not imputed) data.

Analyses were performed with Stata 15.1 (StataCorp, College Station, TX, USA) for descriptive analyses and between-group comparisons, and R 3.4.3 (R Foundation, Vienna, Austria; *pca2d*, *PCAMix*, *Numero*, *mclust* and *NbClust* packages) for clustering analyses and visualizations.

Results

Comparative analyses according to final amyloidosis diagnosis

We included 1394 patients over the 2010-2018 period: 345 (24.7%) had a diagnosis of AL, 263 (18.9%) ATTRv, 402 (28.8%) ATTRwt, and amyloidosis was excluded for 384 (27.5%) patients. **Table 1** and **Figure 1A** show the main clinical and biological characteristics of the studied population as a whole and by final amyloid diagnosis. Overall, ATTRwt patients were older and more predominantly men, with higher prevalence of soft tissue deposition and hearing loss than other patients; ATTRv patients were frequently of Afro-Caribbean or Portuguese origin and frequently presented peripheral neuropathy or soft tissue deposition; AL patients more frequently presented cutaneous and mucosal impairment, dysphonia, and orthostatic and had the most impaired NYHA class and highest NTproBNP/troponin levels. Patients without amyloidosis had a high prevalence of CV risk factors (diabetes, dyslipidemia, hypertension).

Clustering analysis

Figure 2 shows the clustering analysis with the SOM methodology, displaying polarized distributions of patient characteristics across the maps, as evidenced by the contrasting colourings from blue (lowest values) to red (highest values). From these results, seven clusters of patients with homogenous phenotypes were built. Cluster boundaries are shown at the top left of **Figure 2** and as solid black lines across the maps, with detailed characteristics presented in **Table 2**, **Supplemental Table 2** and **Figure 1B**. A summary of the typical characteristics of these seven clusters is in the **Central Illustration**, and a chord diagram in **Figure 3** illustrates the relations between the clinical phenotypes identified by clustering analysis and the CA final diagnosis.

Cluster 1 (N=263, 19%) is located in the upper left area of the maps and included a high proportion of AL patients characterized by impaired CV parameters (highest values of

NTproBNP and troponin and NYHA class and lowest LVEF and strain values) and the highest proportions with underlying gammopathy, microvoltage and skin/mucosal impairment.

Clusters 2 (N=200, 14%), *3* (N=124, 9%) and *4* (N=250, 18%) included patients from the right part of the maps, who were mostly older males with the highest proportions of cardiac fixation on bone scintigraphy and extra-cardiac signs such as soft tissue deposition and hearing loss as well as the highest interventricular septum thickness. Inner subgroups could be identified based on varying proportions of CV risk factors and diseases (i.e., dyslipidemia, hypertension, arrhythmia).

Cluster 2 had high proportions of risk factors and impaired CV parameters, *Cluster 3* had impaired CV parameters with isolated arrhythmia and low proportions of risk factors, and *Cluster 4* conversely showed high proportions of risk factors but preserved CV parameters. Clusters 2 to 4 were all predominantly ATTRwt patients but also included substantial proportions of ATTRv patients (from 21% to 28%).

Clusters 5 (N=149, 11%), *6* (N=230, 16%) and *7* (N=178, 13%), located in the centre and lower left quadrant of the maps, consisted of mostly patients without amyloidosis, with varying phenotypes and overlaps with CA patients. *Cluster 5*, in the centre of the maps, was characterized by older patients with low proportions of CV risk factors and extra-cardiac signs but high proportion of anemia and to a lesser extent peripheral neuropathy and arrhythmia. Patients with this phenotype mostly did not have amyloidosis but also included a moderate proportion of AL patients (25%). *Cluster 6* included patients in the left area of the maps, comprising mostly younger males, with low proportions of CV risk factors and diseases, preserved cardiac function, but remarkably high proportions of peripheral neuropathy and one quarter with Portuguese origin. Patients from *Cluster 6* mostly did not have amyloidosis but also

included a substantial proportion of ATTRv patients with neuropathy (34%). *Cluster 7* comprised patients from the lower left part of the maps, characterized by mostly males about 70 years old with very high proportions of CV risk factors (dyslipidemia, hypertension, diabetes, elevated BMI) but only mildly impaired CV parameters.

Results from the complementary (sensitivity) analysis using model-based clustering identified a seven-cluster solution as the optimal number of clusters, thus confirming the number of clusters found with the SOM approach.

2-D biplot representation (**Figure 4**) illustrates key differences between patients according to their final amyloidosis diagnosis (**Figure 4A**) or cluster by SOMs (**Figure 4B**). As expected, patients diagnosed with AL or from Cluster 1 distinctly projected along variables relating to the typical clinical presentation of the disease (i.e., cutaneous and mucosal impairment, underlying gammopathy, microvoltage). Regarding other diagnoses and clusters, separation of the subgroups was clearer after clustering (**Figure 4B**), which accentuated key differences in phenotypes, than by considering the final diagnosis, with non-amyloidosis patients substantially overlapping with ATTRv patients.

Prognostic analyses

Figure 5 shows results from 4-year overall survival analyses according to the final amyloid diagnosis (**Figure 5A**) or clusters from SOMs (**Figure 5B**). The best survival outcomes were for no-amyloidosis patients and Cluster 6 and the worst outcomes were for AL patients and Clusters 1 and 2 patients, with intermediate results for ATTRwt and ATTRv patients and Cluster 3, 4, 5 and 7 patients. A detailed breakdown of the survival rates at 4-year follow-up for each cluster by amyloid status is provided in **Supplemental Table 3**; results were consistent with the global results, with Clusters 1 and 2 having generally worse outcomes and Cluster 6 generally

better outcomes. Harrell's C-index from a Cox proportional hazards model was substantially higher entering cluster membership (69.0%) than amyloid status (65.5%).

Discussion

To our knowledge, this is the first study using clustering analysis to identify paraclinical presentations depending on phenotypes in a large set of patients with and without amyloidosis. We identified seven distinct clusters with contrasted profiles and prognosis. AL patients were specifically located within a typical cluster; ATTRv patients were distributed across four clusters with varying clinical presentations, one of which overlapping with patients without amyloidosis; remarkably, ATTRwt patients spread across three distinct clusters of older males with contrasted risk factors, biological profiles and prognosis. These results suggest key areas to improve amyloidosis diagnostic skills and stratify patient prognosis, especially within patients with ATTRwt. This issue is of critical importance because the heterogeneity of the disease expression and the lack of early diagnostic tools and knowledge regarding management of amyloidosis can lead to delays in the diagnosis and an aggravation of the prognosis(23). Thus, there is a current need to better characterize the whole spectrum of the disease.

AL patients had a distinct phenotype with poor prognosis

Most AL patients (61%) were in Cluster 1, characterized by severe cardiac amyloidosis with elevated NTproBNP level, clinical signs of heart failure as assessed by higher mean NYHA class, increased LV thickness, low voltage and cardiac involvement on echocardiography, and notably high prevalence of skin/mucosal impairment, peripheral neuropathy and gammopathy. Accordingly, Cluster 1 (along with Cluster 2) had the worst prognosis among the clusters. This finding agrees with the severity of AL disease and its associated poor prognosis, in accordance with previous reports(4). Of note, AL patients were marginally distributed among other clusters,

including within Cluster 5, characterized by older patients with lower NTproBNP level and mostly consisting of patients with no amyloidosis.

ATTRwt patients had heterogenous phenotype and distinct prognosis

Patients with ATTRwt were not found in a single cluster but mostly (89%) spread within three clusters with different prognosis: 29% of all ATTRwt figured in Cluster 2, 20% figured in Cluster 3 and 40% figured in Cluster 4. All three clusters consisted of older males with frequent soft tissue deposition, but Cluster 2 was marked by the highest prevalence of CV risk factors and arrhythmia, with concomitant high cardiac biomarker values and, in turn, the worst prognosis. CV risk factors were also prevalent in Cluster 4, but NTproBNP level was markedly lower, with ultimately better prognosis. These results highlight the heterogeneity of prognosis within patients with ATTRwt amyloidosis and, consequently, the crucial need to assess CV biomarkers and risk factors associated to CA in those patients to inform prognosis and adapt care management.

ATTRwt is under-diagnosed and could represent 13% of heart failure cases in older men (24,25). Age is a major determinant of the risk of cardiovascular disease (26). Main implicated processes include excessive oxidative stress and chronic low-grade inflammation superimposed on the limited cardiac regeneration capacity (26). This situation might explain why patients from Clusters 2 and 4 had a high prevalence of cardiovascular risk factors such as dyslipidemia, hypertension and diabetes. Concerning the severity of the cardiac involvement, Cluster 2 seemed more severe than Cluster 4, with no clear explanation except that Cluster 2 patients were nearly 2 years older than Cluster 4 and more frequently had arrhythmia. Differences in duration of development of the disease might contribute to this discrepancy between the two clusters. In contrast, patients of Cluster 3 with similar mean age as patients from Cluster 2 presented moderately severe cardiac amyloidosis with an intermediate prognosis. These patients had very

few CV risk factors as compared with Cluster 2 patients, which supports the aggravating role that CV risk factors might play and even their potential contribution to the development of ATTRwt amyloidosis(27).

ATTRv patients presented multiple phenotypes

ATTRv patients were widespread across several clusters, including Clusters 6, 4, 2 and 3 representing respectively 30%, 25%, 16% and 13% of ATTRv patients, and showed varying presentations, without a clear emblematic phenotype. This finding is consistent with the previously reported high heterogeneity of the ATTRv phenotype(25), which further highlights how such phenotype heterogeneity may lead to under-diagnosis of ATTRv in real-life settings(8,28). Data currently available indicate an under-diagnosis and reporting of CA pathology, which could represent for ATTR-CA, 8% of hypertrophic cardiomyopathies(25), confirmed in a similar approach in the United States(29). In detail, Cluster 6 had a high proportion of the ATTR V30M mutation (68%) frequently found in patients from Portugal(30). This mutation leads to a mixed phenotype with neuropathy and mild CA. Therefore, in early onset, the disease has mainly a neurologic phenotype and in late onset, a mixed phenotype. Other patients with V30M mutation were in Cluster 2 (30%) and mostly consisted of late-onset patients from European countries other than Portugal(30). The well-described “Afro-American” V122I mutation was spread in Clusters 2, 3, 4, with 30%, 21% and 31% of these patients, respectively.

Patients without amyloidosis

Patients without amyloidosis were mainly found in Cluster 7, which presented a high prevalence of risk factors, in particular obesity (43%), diabetes (77%), dyslipidemia (62%) and hypertension (91%), leading to increased left ventricular mass and potentially misleading the diagnosis of CA. To our knowledge, the diagnostic value for detecting CA of obesity and other

cardiovascular risk factors has not been specifically studied, and further research is needed to investigate this topic. Of note, patients from this cluster were younger than ATTRwt patients from Clusters 2 and 4 and did not present soft tissue deposition. Clusters 5 and 6 also mostly consisted of patients without amyloidosis, with Cluster 6 patients being much younger and having milder cardiac involvement than Cluster 5 patients. Prognosis of these clusters was better than other clusters with more amyloidosis patients.

Comparison of prognosis between clusters

Our clustering analysis allowed for identifying distinct prognostic profiles across clusters, with Clusters 1, 2, and 3 having the poorest outcome; Clusters 4, 5 and 7 intermediate outcome; and Cluster 6 the best outcome. The most affected clusters in terms of prognosis were those with the poorest heart condition, revealed by NTproBNP/troponin levels and cardiologic characteristics such as interventricular septum thickness or strain. Median NTproBNP level for Clusters 1 and 2 was 5300 and 5900 ng/L at inclusion, for instance, which was already about three-fold higher than median NTproBNP level for Clusters 4, 5 and 7. In terms of prognosis, we therefore believe that perhaps what matters most is the heart condition rather than the pathology diagnosed. This was particularly highlighted by the observation that prognosis could actually be worse in some ATTR patients (notably from Cluster 2) than in AL patients.

Strengths

Among the strengths of our study are the use of a large amyloidosis database gathering detailed phenotype information on patients with a final diagnosis of CA but also patients with suspected CA ultimately excluded from that diagnosis, and the use of advanced statistical unsupervised approaches. Use of such machine learning-based algorithms enabled the identification of distinct paraclinical presentations by providing insightful representations of

patient characteristics with blinding to the final diagnosis. In this regard, an interesting aspect of SOMs is the ability to build powerful and user-friendly visualisations of clustering results, allowing to easily capture key similarities and differences but also overlaps between clusters defined, thus highlighting the complexity of the pathology.

Limitations

Our study has also some limitations, including the monocentric nature of the study design, although relying on an extended reference network with a large variety of patients referred. Study limitations also include the fact that some variables used for clustering or illustrative purpose had a substantial amount of missing information, for which we used missing data imputation for the SOM analysis. An interesting future prospect would be to externally validate the key phenotypes identified here in another large prospective cohort. Another interesting perspective to broaden the spectrum of the features investigated would be to enrich current databases from referral centers with information automatically collected from electronic health records, using machine learning techniques to help discover novel clinical or biological markers for early diagnosis and refined prognosis.

Conclusions

Using clustering analysis on a large database of patients with and without cardiac amyloidosis, we identified seven key clinical profiles with distinct characteristics, varying associations with amyloidosis diagnosis and contrasted prognosis, thus contributing to refine risk stratification in patients with amyloidosis. Our findings may help further define both typical clinical presentations but also less evocative situations or signs to ultimately improve amyloidosis diagnostic skills of clinicians. Especially in patients with ATTRwt, our results

suggest key areas to improve amyloidosis diagnosis and stratify prognosis depending on associated CV risk factors.

Clinical perspectives

Competency in Medical Knowledge: The heterogeneous phenotypes of cardiac amyloidosis (CA) contribute to delayed diagnosis and adverse outcomes. A clustering analysis by self-organizing maps of patients with suspected CA identifies seven typical presentations with considerable overlap.

Translational Outlook: Further efforts are needed to facilitate the early diagnosis of CA and guide therapy.

References

1. Kelly JW. Mechanisms of amyloidogenesis. *Nat Struct Biol* 2000;7:824-6.
2. Merlini G, Bellotti V. Molecular mechanisms of amyloidosis. *N Engl J Med* 2003;349:583-96.
3. Buxbaum JN, Tagoe CE. The genetics of the amyloidoses. *Annu Rev Med* 2000;51:543-69.
4. Damy T, Jaccard A, Guellich A et al. Identification of prognostic markers in transthyretin and AL cardiac amyloidosis. *Amyloid* 2016;23:194-202.
5. Seward JB, Casacang-Verzosa G. Infiltrative cardiovascular diseases: cardiomyopathies that look alike. *J Am Coll Cardiol* 2010;55:1769-79.
6. Di Bella G, Pizzino F, Minutoli F et al. The mosaic of the cardiac amyloidosis diagnosis: role of imaging in subtypes and stages of the disease. *Eur Heart J Cardiovasc Imaging* 2014;15:1307-15.
7. Damy T, Maurer MS, Rapezzi C et al. Clinical, ECG and echocardiographic clues to the diagnosis of TTR-related cardiomyopathy. *Open Heart* 2016;3:e000289.
8. Witteles RM, Bokhari S, Damy T et al. Screening for Transthyretin Amyloid Cardiomyopathy in Everyday Practice. *JACC Heart Fail* 2019;7:709-716.
9. Authors/Task Force m, Elliott PM, Anastakis A et al. 2014 ESC Guidelines on diagnosis and management of hypertrophic cardiomyopathy: the Task Force for the Diagnosis and Management of Hypertrophic Cardiomyopathy of the European Society of Cardiology (ESC). *Eur Heart J* 2014;35:2733-79.
10. Kelly JJ, Jr., Kyle RA, O'Brien PC, Dyck PJ. The natural history of peripheral neuropathy in primary systemic amyloidosis. *Ann Neurol* 1979;6:1-7.

11. Sperry BW, Reyes BA, Ikram A et al. Tenosynovial and Cardiac Amyloidosis in Patients Undergoing Carpal Tunnel Release. *J Am Coll Cardiol* 2018;72:2040-2050.
12. Donnelly JP, Hanna M, Sperry BW, Seitz WH, Jr. Carpal Tunnel Syndrome: A Potential Early, Red-Flag Sign of Amyloidosis. *J Hand Surg Am* 2019;44:868-876.
13. Bequignon E, Guellich A, Barthier S et al. How your ears can tell what is hidden in your heart: wild-type transthyretin amyloidosis as potential cause of sensorineural hearing loss in elderly-AmyloDEAFNESS pilot study. *Amyloid* 2017;24:96-100.
14. Bartier S, Bodez D, Kharoubi M et al. Pharyngo-laryngeal involvement in systemic amyloidosis with cardiac involvement: a prospective observational study. *Amyloid* 2019;26:216-224.
15. Kumar S, Sengupta RS, Kakkar N, Sharma A, Singh S, Varma S. Skin involvement in primary systemic amyloidosis. *Mediterr J Hematol Infect Dis* 2013;5:e2013005.
16. Gertz MA, Dispenzieri A. Systemic Amyloidosis Recognition, Prognosis, and Therapy: A Systematic Review. *JAMA* 2020;324:79-89.
17. Volzke H, Schmidt CO, Baumeister SE et al. Personalized cardiovascular medicine: concepts and methodological considerations. *Nat Rev Cardiol* 2013;10:308-16.
18. Kyle RA, Therneau TM, Rajkumar SV et al. Prevalence of monoclonal gammopathy of undetermined significance. *N Engl J Med* 2006;354:1362-9.
19. Dispenzieri A, Gertz MA, Kyle RA et al. Serum cardiac troponins and N-terminal pro-brain natriuretic peptide: a staging system for primary systemic amyloidosis. *J Clin Oncol* 2004;22:3751-7.
20. Kohonen T, Somervuo P. How to make large self-organizing maps for nonvectorial data. *Neural Netw* 2002;15:945-52.

21. Gao S, Mutter S, Casey A, Makinen VP. Numero: a statistical framework to define multivariable subgroups in complex population-based datasets. *Int J Epidemiol* 2018.
22. Fraley C, Raftery AE. Model-based clustering, discriminant analysis, and density estimation. *Journal of the American statistical Association* 2002;97:611-631.
23. Gertz M, Adams D, Ando Y et al. Avoiding misdiagnosis: expert consensus recommendations for the suspicion and diagnosis of transthyretin amyloidosis for the general practitioner. *BMC family practice* 2020;21:198.
24. Mohty D, Pradel S, Magne J et al. Prevalence and prognostic impact of left-sided valve thickening in systemic light-chain amyloidosis. *Clin Res Cardiol* 2017;106:331-340.
25. Damy T, Costes B, Hagege AA et al. Prevalence and clinical phenotype of hereditary transthyretin amyloid cardiomyopathy in patients with increased left ventricular wall thickness. *Eur Heart J* 2016;37:1826-34.
26. Triposkiadis F, Xanthopoulos A, Butler J. Cardiovascular Aging and Heart Failure: JACC Review Topic of the Week. *J Am Coll Cardiol* 2019;74:804-813.
27. Gonzalez-Lopez E, Gallego-Delgado M, Guzzo-Merello G et al. Wild-type transthyretin amyloidosis as a cause of heart failure with preserved ejection fraction. *Eur Heart J* 2015;36:2585-94.
28. Maurer MS, Bokhari S, Damy T et al. Expert Consensus Recommendations for the Suspicion and Diagnosis of Transthyretin Cardiac Amyloidosis. *Circulation Heart failure* 2019;12:e006075.
29. Akinboboye O, Shah K, Warner AL et al. DISCOVERY: prevalence of transthyretin (TTR) mutations in a US-centric patient population suspected of having cardiac amyloidosis. *Amyloid* 2020:1-8.

30. Damy T, Kristen AV, Suhr OB et al. Transthyretin cardiac amyloidosis in continental Western Europe: an insight through the Transthyretin Amyloidosis Outcomes Survey (THAOS). Eur Heart J 2019.

Figure legends

Figure 1. Distribution of patient characteristics by amyloid status and clusters. Data are shown (A) by amyloid status and (B) by clusters identified by self-organizing maps (SOM).

Results are displayed as boxplots, with the horizontal line indicates the median, box edges the interquartile range, and whiskers extending to 1.5 times the interquartile range above and below the box; the dots represent individual patients.

Figure 2. Results from the clustering analysis by self-organizing maps. - Left part: based on expert-driven visual identification of key patterns in the self-organizing maps (SOM) on the right, close districts were combined to provide seven suitable clusters of patients. Cluster boundaries are delimited by solid black lines.- Right part: unsupervised analysis by SOM placed all patients identified as globally similar for clinical and paraclinical parameters in 1 of 66 small groupings (“districts”) throughout the map. The more patients were similar in terms of global phenotyping, the closer they are placed on the map. Each individual map shows the mean values or proportions per district for each characteristic; blue indicates the lowest average values and red the highest, with detailed numbers shown for a selection of representative districts in each SOM. BMI: body mass index; IST: interventricular septum thickness; LV: left ventricle; LVEF: LV ejection fraction; NYHA: New York Heart Association classification; SBP: systolic blood pressure.

Figure 3. Chord diagram of the relations between amyloid status and clusters. Illustrates the proportions of the typical presentations identified by clustering analysis (on the right) by cardiac amyloidosis final diagnosis (on the left). For the sake of readability, only percentages above 10% are shown and results are presented separately for patients with (A) no amyloidosis, (B) ATTRv, (C) ATTRwt and (D) AL amyloidosis.

Figure 4. Biplot representations of patients characteristics by amyloid status and clusters.

The biplot representation of the 24 variables retained as characteristic parameters, allowing for visualization of the relations between variables used for building clusters (arrows) while simultaneously displaying the patients (dots), based on their individual characteristics. Results are projected onto the 2 first dimensions (PC1, PC2) generated by principal component analysis. Colours for observations correspond to the final amyloidosis status diagnosed (A) or to the seven-group solution from cluster analysis (B).

Figure 5. Kaplan-Meier overall survival curves according to amyloid status and clusters.

Survival curves for 4-year overall survival are plotted by (A) amyloid status and (B) clusters using the Kaplan-Meier method. Numbers of patients at risk and number of events are shown in the risk table below the graph.

Central Illustration. Summary of the main characteristics of the seven phenotypic profiles (clusters) revealed by the clustering analysis. The clustering analysis by self-organizing maps revealed seven typical phenotypic profiles (clusters) with distinct clinical presentations and prognosis. A simplified summary of the main characteristics of the clusters is given in the table, where colors intensity semiquantitatively represent the magnitude (frequency or quantitative level) of each attribute. The prognostic value of the clusters is highlighted by the differentiated Kaplan-Meier survival curves for 4-year overall survival.

Video Legend

Video 1. 3-D biplot according to the clusters identified by SOMs. 3-D biplot visualizations based on mixed principal component analysis illustrate the differentiated distribution of clinical and paraclinical characteristics (displayed as arrows) across the seven clusters of patients (displayed as dots).

Table 1. Main characteristics of patients overall and by amyloid status

	N complete d	Total N=1394	No amyloidosis N=384	AL N=345	ATTRv N=263	ATTRwt N=402	
Clinical characteristics							
Age at inclusion, years	1394	71.5 ±13.2	68.3 ±14.9	66.9 ±11.4	67.9 ±12.6	81.0 ±7.3	
Sex, men	1394	984 (70.6%)	242 (63.0%)	214 (62.0%)	176 (66.9%)	352 (87.6%)	
Ethnicity/country of origin							
	Caucasian	695	447 (64.3%)	28 (50.0%)	130 (69.1%)	51 (28.7%)	238 (87.2%)
	Afro-Caribbean		65 (9.4%)	6 (10.7%)	10 (5.3%)	44 (24.7%)	5 (1.8%)
	Northern Africa		120 (17.3%)	19 (33.9%)	31 (16.5%)	55 (30.9%)	15 (5.5%)
	Portuguese		53 (7.6%)	2 (3.6%)	13 (6.9%)	25 (14.0%)	13 (4.8%)
	Other		10 (1.4%)	1 (1.8%)	4 (2.1%)	3 (1.7%)	2 (0.7%)
Body mass index, kg/m ²		25.2 (±4.7)	26.8 (±6.2)	24.1 (±4.2)	24.5 (±4.0)	25.4 (±3.6)	
	Continuous	1236					
	≥ 30		163 (13.2%)	66 (22.1%)	29 (9.0%)	20 (8.7%)	48 (12.6%)
Diabetes	1394	269 (19.3%)	116 (30.2%)	48 (13.9%)	39 (14.8%)	66 (16.4%)	
Dyslipidemia	1394	425 (30.5%)	128 (33.3%)	92 (26.7%)	55 (20.9%)	150 (37.3%)	
Hypertension	1394	706 (50.6%)	238 (62.0%)	127 (36.8%)	109 (41.4%)	232 (57.7%)	

Anemia		1298	589 (42.3%)	183 (47.7%)	173 (50.1%)	94 (35.7%)	139 (34.6%)
Amyloidosis symptoms							
Cutaneous and mucosal impairment		1394	214 (15.4%)	4 (1.0%)	124 (35.9%)	35 (13.3%)	51 (12.7%)
Soft tissue deposition		1394	523 (37.5%)	27 (7.0%)	72 (20.9%)	144 (54.8%)	280 (69.7%)
Peripheral neuropathy		1394	668 (47.9%)	188 (49.0%)	150 (43.5%)	193 (73.4%)	137 (34.1%)
Hearing loss		1394	343 (24.6%)	13 (3.4%)	58 (16.8%)	67 (25.5%)	205 (51.0%)
Amyloidosis characterization							
ATTR mutation		998	260 (26.1%)	0 (0.0%)	1 (0.6%)	259 (100.0%)	0 (0.0%)
Genotype	No mutation	998	738 (73.9%)	196 (100.0%)	154 (99.4%)	0 (0.0%)	388 (100.0%)
	Val122Ile		116 (11.6%)	0 (0.0%)	0 (0.0%)	116 (44.8%)	0 (0.0%)
	Val30Met		65 (6.5%)	0 (0.0%)	0 (0.0%)	65 (25.1%)	0 (0.0%)
	Other mutation*		79 (7.9%)	0 (0.0%)	1 (0.6%)	78 (30.1%)	0 (0.0%)
Cardiac fixation on bone scintigraphy		940	547 (58.2%)	1 (0.5%)	23 (11.4%)	160 (85.6%)	363 (98.9%)
Underlying gammopathy		1394	477 (34.2%)	35 (9.1%)	345 (100.0%)	18 (6.8%)	79 (19.7%)
Hemodynamics and cardiology characteristics							
NYHA class	I	1394	281 (20.2%)	119 (31.0%)	39 (11.3%)	70 (26.6%)	53 (13.2%)
	II		559 (40.1%)	137 (35.7%)	125 (36.2%)	107 (40.7%)	190 (47.3%)

	III		437 (31.3%)	94 (24.5%)	139 (40.3%)	73 (27.8%)	131 (32.6%)
	IV		117 (8.4%)	34 (8.9%)	42 (12.2%)	13 (4.9%)	28 (7.0%)
EKG low voltage		1394	380 (27.3%)	66 (17.2%)	156 (45.2%)	70 (26.6%)	88 (21.9%)
Atrial arrhythmia		1394	294 (21.1%)	57 (14.8%)	39 (11.3%)	38 (14.4%)	160 (39.8%)
Pacemaker or ICD		1146	130 (11.3%)	33 (12.1%)	17 (5.7%)	19 (9.0%)	61 (16.7%)

Data are mean (\pm standard deviation) for continuous variables and n (%) for categorical variables, unless otherwise stated.

AL, light-chain amyloidosis; ATTRv, hereditary variant transthyretin amyloidosis; ATTRwt, wild-type transthyretin amyloidosis; ECG, electrocardiography; ICD, implantable cardioverter-defibrillator; IQR: interquartile range; NYHA, New York Heart Association

All p-values from global comparisons across amyloid status categories <0.0001

* Other mutations with 5 or more patients include Ser77Tyr, Ile107Val, Ser77Phe, Ile68Leu

Table 2. Main characteristics of patients according to clusters identified by self-organizing maps (SOMs)

		Cluster 1	Cluster 2	Cluster 3	Cluster 4	Cluster 5	Cluster 6	Cluster 7
		N=263	N=200	N=124	N=250	N=149	N=230	N=178
Clinical characteristics								
Age at inclusion, years		65.2 ±11.5	79.8 ±7.8	79.0 ±8.4	77.3 ±8.1	78.3 ±11.3	58.1 ±13.6	70.0 ±11.1
Sex, men		149 (56.7%)	172 (86.0%)	106 (85.5%)	210 (84.0%)	76 (51.0%)	147 (63.9%)	124 (69.7%)
Ethnicity/country of origin	Caucasian	108 (74.0%)	58 (60.4%)	64 (71.9%)	133 (68.9%)	28 (53.8%)	31 (45.6%)	25 (49.0%)
	Afro-Caribbean	8 (5.5%)	12 (12.5%)	11 (12.4%)	16 (8.3%)	4 (7.7%)	6 (8.8%)	8 (15.7%)
	Northern Africa	19 (13.0%)	21 (21.9%)	12 (13.5%)	27 (14.0%)	16 (30.8%)	12 (17.6%)	13 (25.5%)
	Portuguese	7 (4.8%)	5 (5.2%)	1 (1.1%)	14 (7.3%)	4 (7.7%)	18 (26.5%)	4 (7.8%)
	Other	4 (2.7%)	0 (0.0%)	1 (1.1%)	3 (1.6%)	0 (0.0%)	1 (1.5%)	1 (2.0%)
Body mass index, kg/m ²	Continuous	23.7 ±4.0	24.8 ±3.9	25.3 ±4.1	25.8 ±3.2	23.1 ±3.8	24.6 ±3.7	29.6 ±7.1
	≥ 30	17 (7.0%)	21 (11.5%)	17 (14.3%)	27 (11.2%)	5 (4.0%)	10 (6.0%)	66 (42.6%)
Diabetes		24 (9.1%)	28 (14.0%)	6 (4.8%)	56 (22.4%)	7 (4.7%)	11 (4.8%)	137 (77.0%)
Dyslipidemia		48 (18.3%)	84 (42.0%)	8 (6.5%)	123 (49.2%)	23 (15.4%)	28 (12.2%)	111 (62.4%)
Hypertension		69 (26.2%)	122 (61.0%)	40 (32.3%)	180 (72.0%)	80 (53.7%)	53 (23.0%)	162 (91.0%)
Anemia		124 (47.1%)	96 (48.0%)	29 (23.4%)	75 (30.0%)	106 (71.1%)	63 (27.4%)	96 (53.9%)
Amyloidosis symptoms								
Cutaneous and mucosal impairment		124 (47.1%)	23 (11.5%)	15 (12.1%)	40 (16.0%)	0 (0.0%)	8 (3.5%)	4 (2.2%)
Soft tissue deposition		59 (22.4%)	101 (50.5%)	107 (86.3%)	186 (74.4%)	17 (11.4%)	36 (15.7%)	17 (9.6%)
Peripheral neuropathy		131 (49.8%)	82 (41.0%)	32 (25.8%)	122 (48.8%)	75 (50.3%)	164 (71.3%)	62 (34.8%)

Hearing loss		40 (15.2%)	63 (31.5%)	70 (56.5%)	140 (56.0%)	8 (5.4%)	12 (5.2%)	10 (5.6%)
Amyloidosis characterization								
Amyloid status	No amyloidosis	13 (4.9%)	27 (13.5%)	3 (2.4%)	12 (4.8%)	75 (50.3%)	122 (53.0%)	132 (74.2%)
	AL	230 (87.5%)	15 (7.5%)	2 (1.6%)	12 (4.8%)	37 (24.8%)	26 (11.3%)	23 (12.9%)
	ATTRv	12 (4.6%)	43 (21.5%)	35 (28.2%)	67 (26.8%)	17 (11.4%)	78 (33.9%)	11 (6.2%)
	ATTRwt	8 (3.0%)	115 (57.5%)	84 (67.7%)	159 (63.6%)	20 (13.4%)	4 (1.7%)	12 (6.7%)
ATTR mutation		11 (8.1%)	44 (25.1%)	34 (28.6%)	66 (28.0%)	17 (20.2%)	77 (53.1%)	11 (10.6%)
Genotype	Negative	124 (91.9%)	131 (74.9%)	85 (71.4%)	170 (72.0%)	67 (79.8%)	68 (46.9%)	93 (89.4%)
	V122I	0 (0.0%)	35 (20.0%)	24 (20.2%)	36 (15.3%)	9 (10.7%)	5 (3.4%)	7 (6.7%)
	V30M	0 (0.0%)	0 (0.0%)	0 (0.0%)	16 (6.8%)	5 (6.0%)	44 (30.3%)	0 (0.0%)
	Other	11 (8.1%)	9 (5.1%)	10 (8.4%)	14 (5.9%)	3 (3.6%)	28 (19.3%)	4 (3.8%)
Cardiac fixation on bone scintigraphy		30 (18.4%)	140 (92.1%)	107 (98.2%)	211 (97.2%)	23 (24.2%)	17 (17.3%)	19 (17.9%)
Underlying gammopathy		243 (92.4%)	50 (25.0%)	16 (12.9%)	44 (17.6%)	48 (32.2%)	37 (16.1%)	39 (21.9%)
Hemodynamics and cardiology characteristics								
NYHA class	I	14 (5.3%)	14 (7.0%)	13 (10.5%)	41 (16.4%)	16 (10.7%)	149 (64.8%)	34 (19.1%)
	II	75 (28.5%)	32 (16.0%)	67 (54.0%)	153 (61.2%)	95 (63.8%)	64 (27.8%)	73 (41.0%)
	III	132 (50.2%)	93 (46.5%)	43 (34.7%)	56 (22.4%)	33 (22.1%)	16 (7.0%)	64 (36.0%)
	IV	42 (16.0%)	61 (30.5%)	1 (0.8%)	0 (0.0%)	5 (3.4%)	1 (0.4%)	7 (3.9%)
EKG low voltage		147 (55.9%)	48 (24.0%)	17 (13.7%)	61 (24.4%)	23 (15.4%)	53 (23.0%)	31 (17.4%)
Atrial arrhythmia		30 (11.4%)	122 (61.0%)	58 (46.8%)	26 (10.4%)	32 (21.5%)	5 (2.2%)	21 (11.8%)
Pacemaker or ICD implant		12 (5.2%)	35 (19.3%)	24 (21.8%)	22 (9.5%)	18 (15.4%)	5 (3.5%)	14 (10.5%)

Data are mean (\pm SD) for continuous variables and n (%) for categorical variables, unless otherwise stated.

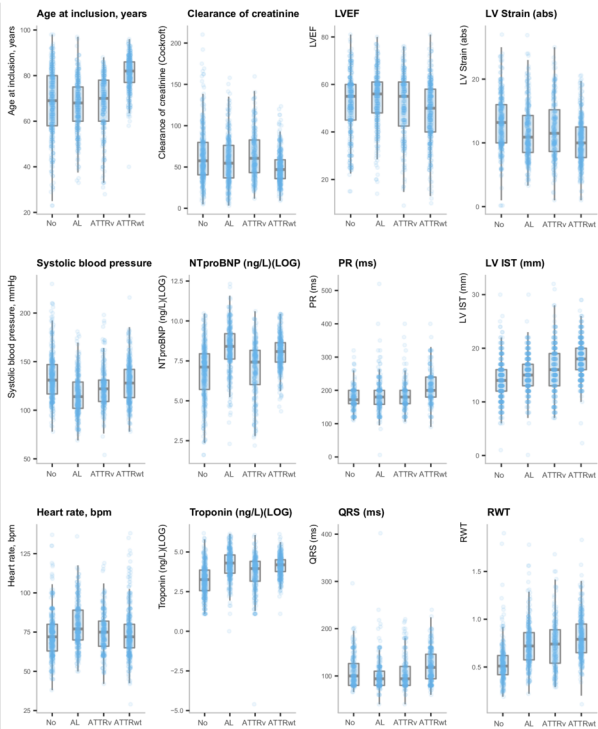
AL, light-chain amyloidosis; ATTRv, hereditary variant transthyretin amyloidosis; ATTRwt, wild-type transthyretin amyloidosis;

ECG, electrocardiography; ICD, implantable cardioverter-defibrillator; IQR: interquartile range; NYHA, New York Heart Association

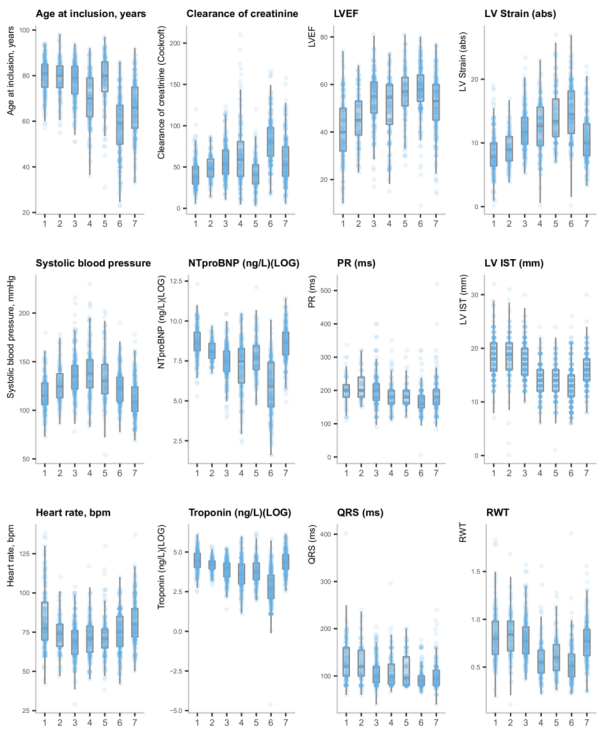
All p-values from global comparisons across clusters <0.0001

* Other mutations with ≥ 5 patients include Ser77Tyr, Ile107Val, Ser77Phe, Ile68Leu.

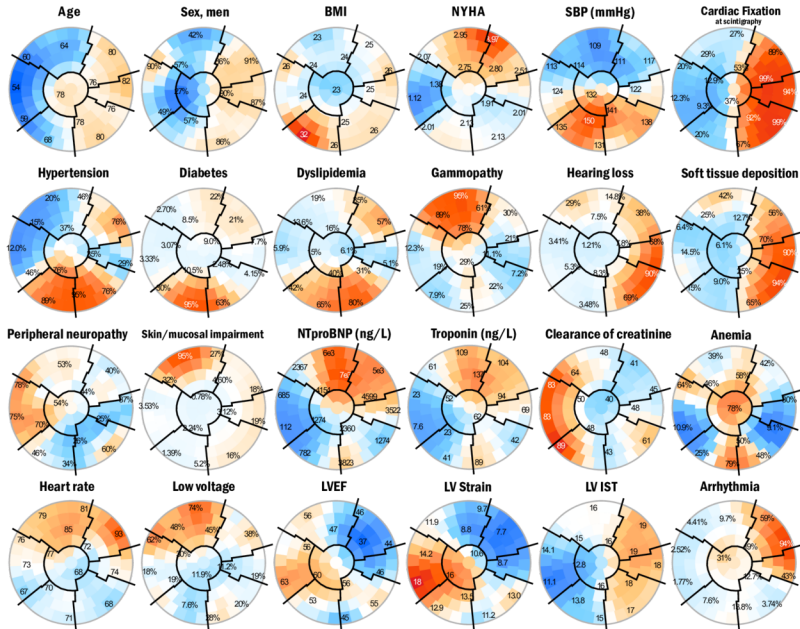
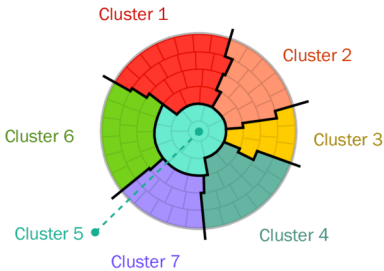
A. By amyloid status



B. By clusters (N=7)

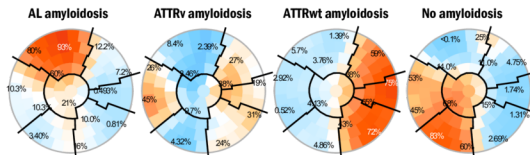


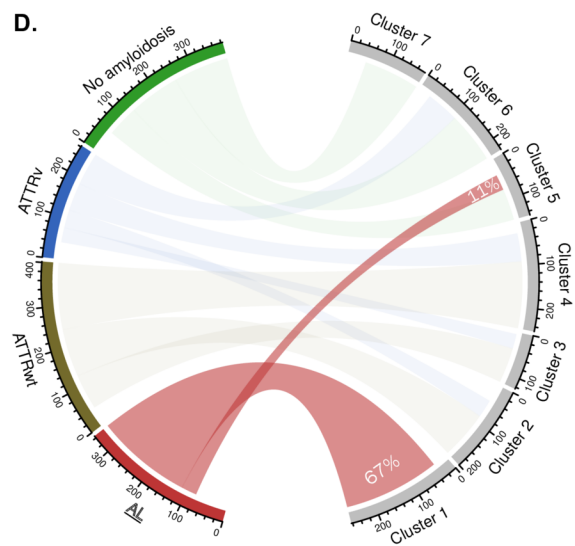
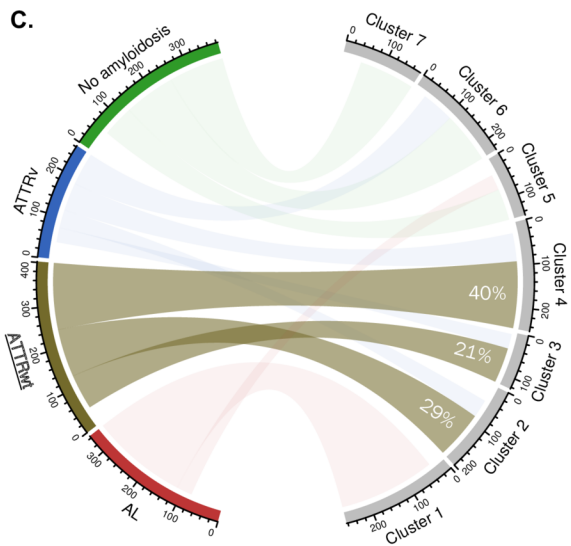
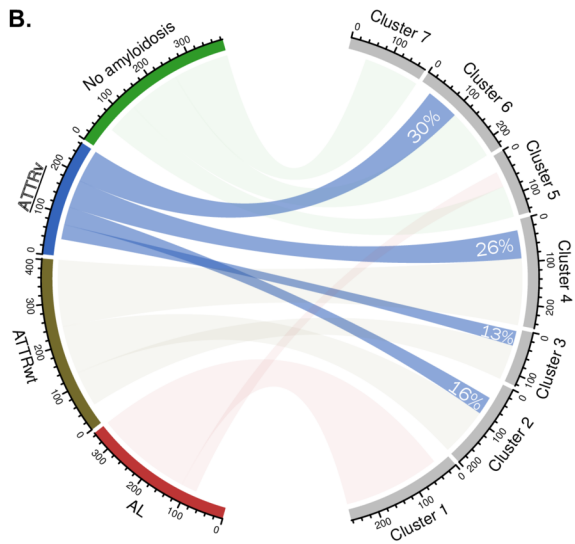
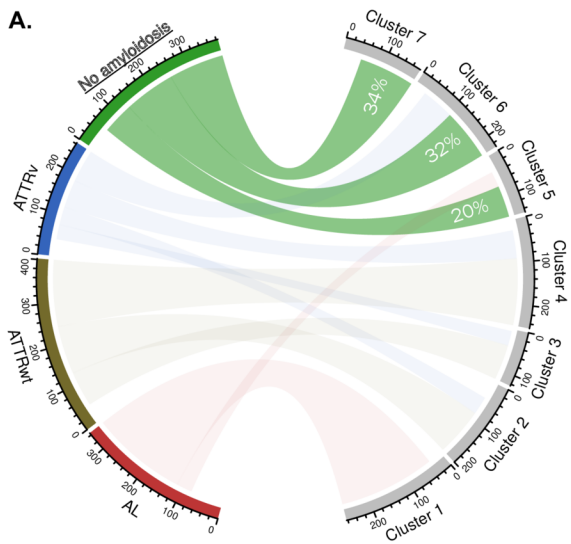
Clusters



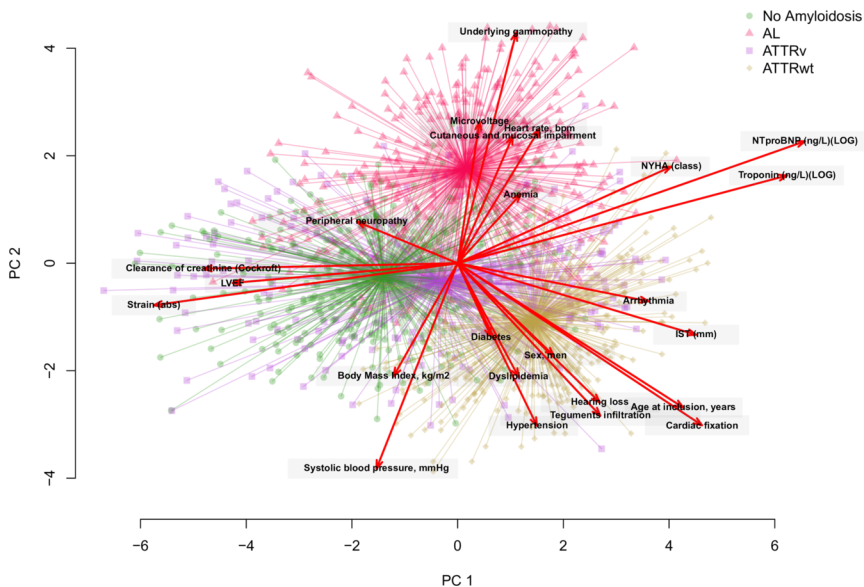
Illustrative features

Final diagnosis

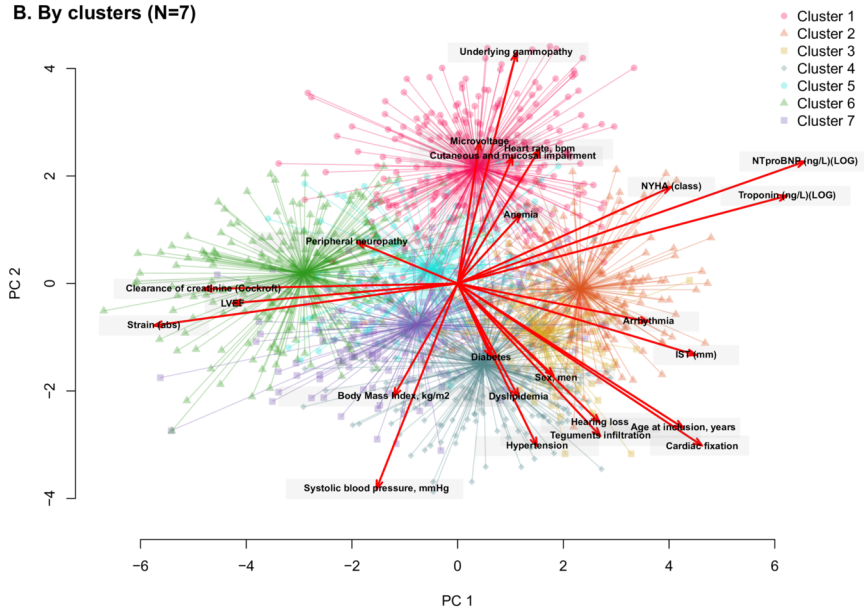




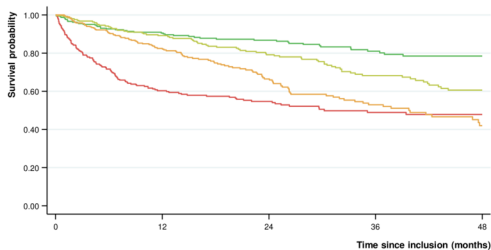
A. By final amyloid status



B. By clusters (N=7)



A. By amyloid status

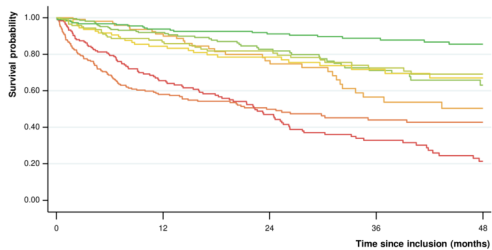


Number at risk (events)

	0	12	24	36	48
No Amyloidosis	327	202	165	101	67
AL	322	132	92	53	40
ATTRv	252	188	137	91	65
ATTRwt	377	204	109	60	27

— No Amyloidosis — AL
— ATTRv — ATTRwt

B. By clusters (N=7)



Number at risk (events)

	0	12	24	36	48
Cluster 1	252	97	64	35	1
Cluster 2	186	87	52	29	8
Cluster 3	116	75	43	22	2
Cluster 4	235	145	87	49	4
Cluster 5	131	76	54	33	2
Cluster 6	200	155	131	91	3
Cluster 7	158	91	72	46	2

— Cluster 1 — Cluster 2 — Cluster 3
— Cluster 4 — Cluster 5 — Cluster 6
— Cluster 7

